

Available online at www.sciencedirect.com

ScienceDirect

www.elsevier.com/locate/jes

JES
 JOURNAL OF
 ENVIRONMENTAL
 SCIENCES
www.jesc.ac.cn

Coating independent cytotoxicity of citrate- and PEG-coated silver nanoparticles on a human hepatoma cell line

Verónica Bastos¹, José M.P. Ferreira-de-Oliveira¹, Joana Carrola², Ana L. Daniel-da-Silva², Iola F. Duarte², Conceição Santos^{3,*}, Helena Oliveira¹

1. CESAM & Laboratory of Biotechnology and Cytomics, Department of Biology, University of Aveiro, 3810-193 Aveiro, Portugal.

E-mail: veronicabastos@ua.pt

2. CICECO — Aveiro Institute of Materials, Department of Chemistry, University of Aveiro, 3810-193 Aveiro, Portugal

3. Department of Biology, Faculty of Sciences, University of Porto, 4169-007 Porto, Portugal

ARTICLE INFO

Article history:

Received 16 March 2016

Revised 21 May 2016

Accepted 28 May 2016

Available online 13 July 2016

Keywords:

Silver nanoparticles (AgNPs)

Citrate

Poly(ethylene glycol) (PEG)

HepG2 cells

Cytotoxicity

Nanotoxicology

ABSTRACT

The antibacterial potential of silver nanoparticles (AgNPs) resulted in their increasing incorporation into consumer, industrial and biomedical products. Therefore, human and environmental exposure to AgNPs (either as an engineered product or a contaminant) supports the emergent research on the features conferring them different toxicity profiles. In this study, 30 nm AgNPs coated with citrate or poly(ethylene glycol) (PEG) were used to assess the influence of coating on the effects produced on a human hepatoma cell line (HepG2), namely in terms of viability, apoptosis, apoptotic related genes, cell cycle and cyclins gene expression. Both types of coated AgNPs decreased cell proliferation and viability with a similar toxicity profile. At the concentrations used (11 and 5 $\mu\text{g}/\text{mL}$ corresponding to IC₅₀ and \sim IC₁₀ levels, respectively) the amount of cells undergoing apoptosis was not significant and the apoptotic related genes *BCL2* (anti-apoptotic gene) and *BAX* (pro-apoptotic gene) were both downregulated. Moreover, both AgNPs affected HepG2 cell cycle progression at the higher concentration (11 $\mu\text{g}/\text{mL}$) by increasing the percentage of cells in S (synthesis phase) and G2 (Gap 2 phase) phases. Considering the cell-cycle related genes, the expression of cyclin B1 and cyclin E1 genes were decreased. Thus, this work has shown that citrate- and PEG-coated AgNPs impact on HepG2 apoptotic gene expression, cell cycle dynamics and cyclin regulation in a similar way. More research is needed to determine the properties that confer AgNPs at lower toxicity, since their use has proved helpful in several industrial and biomedical contexts.

© 2016 The Research Center for Eco-Environmental Sciences, Chinese Academy of Sciences.

Published by Elsevier B.V.

Introduction

AgNPs (silver nanoparticles) are being extensively used in a wide range of applications, from medicine and industry to the most common consumer products (Behra et al., 2013; Eckhardt et al., 2013; Franci et al., 2015; Rai et al., 2015). Consequently, the possible risks associated with their release

into the environment and human exposure has also increased. Indeed, while researchers have stressed the need to establish whether the presence of nanosilver in those products is essential (Nowack and Bucheli, 2007), and several studies showed the toxic potential of AgNPs, their usage remains widespread (Chen et al., 2015; Dusinska et al., 2013; McShan et al., 2014).

* Corresponding author. E-mail: csantos@fc.up.pt (Conceição Santos).

Previous studies have shown that the physico-chemical characteristics of AgNPs will influence cellular uptake, intracellular fate and, consequently, the toxicity of these NPs (Caballero-Díaz et al., 2013; Gliga et al., 2014; Wang et al., 2014; Zhang et al., 2014, 2015). In particular, the size (Gluga et al., 2014; Kim et al., 2012; Park et al., 2011) and surface chemistry (Lu et al., 2010), as well as the type of formulation (Boonkaew et al., 2014), period of exposure (Comfort et al., 2014) and storage conditions (Ahlberg et al., 2014) have all been shown to play a determinant role in AgNPs toxicity.

AgNPs are often coated to promote stability and avoid aggregation. Citrate is the most common reducing agent used to stabilize AgNPs, providing the particles a negative surface charge (Gutierrez et al., 2015; Pillai and Kamat, 2004; Sharma et al., 2009). Polyethylene glycol (PEG) is another popular coating, especially concerning biomedical applications, due to its biocompatible nature and the high stability conferred to the particles (Ryan et al., 2008; Fernández-López et al., 2009). Ginn et al. (2014) refer that in the years to come we will see an increase in the number of novel site-directed PEGylation chemistries and a shift in its application to a wider range of therapeutic molecules, including NPs for therapeutic and diagnostic purposes, becoming essential more studies with this coating. PEG coating improved the biopharmaceutical properties of drugs, increased stability and resistance to proteolytic inactivation, increased circulatory lives, and showed low toxicity (Ginn et al., 2014; Jain and Jain, 2008; Ryan et al., 2008). Moreover, it has been argued that PEG coating decreases AgNPs toxicity by reducing their cellular uptake (Brandenberger et al., 2010; Caballero-Díaz et al., 2013; Pang et al., 2016).

As liver is the most important organ for xenobiotic metabolism (Roberts et al., 2014), liver cell lines have been amply used in biomedical research involving the testing of drugs or other toxicants. The cytotoxicity of AgNPs towards liver cells has also been demonstrated in a few previous studies. Faedmaleki et al. (2014) showed that 20–40 nm AgNPs decreased HepG2 viability in a concentration-dependent manner. Also, Nowrouzi et al. (2010) studied the cytotoxicity of AgNPs on HepG2 and obtained IC50 value of 2.75–3.0 µg/mL for HepG2 after exposure to 5–10 nm AgNPs. Moreover, by determining changes in the activity of lactate dehydrogenase, alanine aminotransferase, aspartate aminotransferase, glutathione peroxidase, superoxide dismutase, lipid peroxidation and cytochrome c content, that same work provided evidence for the involvement of oxidative alterations upon exposure to low doses of AgNPs. Recently, Xin et al. (2015) also found dose-dependent cytotoxicity of AgNPs in HepG2 cells, which was attributed to the interplay of oxidative stress, DNA damage and mitochondrial injury. Consistently, Xue et al. (2016), suggested the cellular toxicological mechanism of AgNPs to be related with oxidative stress induced by the generation of reactive oxygen species (ROS), leading to mitochondria injury and induction of apoptosis. However, there are few studies comparing the coating influence on AgNPs cytotoxicity to liver cells. Kennedy et al. (2014) studied the cytotoxicity potential of carbohydrate functionalization of ~54 nm AgNPs to HepG2 and neuronal-line Neuro 2A cells and found that particles functionalized with ethylene glycol, glucose and citrate coated nanoparticles show a similar toxicity, while galactose and mannose functionalized AgNPs were significantly less toxic to HepG2 cell line. Other studies comparing the influence of coating on AgNPs cytotoxicity have been addressed

to other cell lines. Gluga et al. (2014) compared the cytotoxicity of uncoated, PVP- and citrate-coated AgNPs in bronchial BEAS-2B cells and found no coating-dependent differences in cytotoxicity. Caballero-Díaz et al. (2013) reported that pegylation of AgNPs reduced cellular uptake and reduced the toxicity in NIH/3T3 (mouse embryonic fibroblasts), compared to AgNPs coated with other polymers. The conflicting existing information addressed the need to deeply study surface coating AgNPs cytotoxicity, in order to be aware if or which nanoparticles (NPs) are more cytotoxic to the different cell lines.

In this study we aimed to compare the influence of coating (citrate vs. PEG) on the cytotoxicity of AgNPs in liver cells, using the human hepatoma cell line HepG2 as an *in vitro* model. HepG2 cells were exposed to citrate- and PEG-coated AgNPs of 30 nm diameter and the effects on cell viability, apoptosis induction, apoptotic expression genes, cell cycle profile and cyclins gene expression were assessed.

1. Material and methods

1.1. Chemicals

Sterile, purified and endotoxin-free AgNPs (Biopure AgNPs 1.0 mg/mL), with 30-nm diameter and a citrate or PEG surface, designated from now on as Cit30 and PEG30 NPs, were purchased from Nanocompositix Europe (Prague, Czech Republic). Citric acid (C₆H₈O₇·H₂O) was purchased from Sigma Aldrich (St. Louis, Missouri, USA); PEG (MW 5 kDa) from Laysan Bio® (Arab, Alabama, USA) and silver nitrate reagent (AgNO₃) from Sigma Aldrich (St. Louis, MO, USA). Dulbecco's modified Eagle's medium (DMEM), fetal bovine serum (FBS), antibiotics and phosphate buffer saline (PBS, pH 7.4) were purchased from Life Technologies (Carlsbad, CA, USA). 3-(4,5-Dimethylthiazol-2-yl)-2,5-diphenyltetrazolium bromide (MTT) and dimethyl sulfoxide (DMSO) were obtained from Sigma-Aldrich (St. Louis, MO, USA). RNase and propidium iodide (PI) were both from Sigma-Aldrich, St. Louis, MO-USA.

1.2. Physicochemical characterization of AgNPs

The morphology and size of AgNPs was assessed by scanning transmission electron microscopy (STEM) using a scanning electron microscope Hitachi SU-70 (Hitachi High-Technologies Europe GmbH, Germany) operating at 30 kV. Samples for STEM analysis were prepared by evaporating dilute suspensions of the nanoparticles on a copper grid coated with an amorphous carbon film. The hydrodynamic diameter and polydispersity index (PDI) of the nanoparticles were measured by dynamic light scattering (DLS) and the zeta potential was assessed by electrophoretic mobility, both measurements using a Zetasizer Nano ZS (Malvern Instruments, UK).

Silver quantification measurements were performed by inductively coupled plasma optical emission spectrometry (ICP-OES) in an Activa M Radial spectrometer (Horiba Jobin Yvon), employing a charge coupled device (CCD) array detector, with a wavelength range of 166–847 nm and radial plasma view. Samples were introduced into the ICP plasma using an HF resistant sample introduction system including a Burgener nebulizer, a cyclonic spray chamber and a quartz

torch with aluminum injector. Samples for ICP-OES were prepared by addition of 10 μL AgNPs (1.0 mg/mL) to 990 μL of either ultrapure water or complete culture medium, incubation for variable periods (0, 4, 24 or 48 hr), followed by centrifugation at 40,000 $\times g$ for 120 min at 4°C (in accordance with the manufacturer's recommendations) to deposit the nanoparticles and separate the supernatant (with dissolved ionic silver). Acid digestion of the supernatant was then performed by mixing 500 μL with 100 μL of acids (HCl:HNO₃, 2:1, V/V) and 400 μL of ultrapure water. The % dissolution of AgNPs to ionic silver was calculated as $100 \times F \times C_{\text{Ag}}/C_i$, where F is the dilution factor, C_i the initial concentration of AgNPs and C_{Ag} the concentration of silver determined by ICP-OES.

1.3. Cell culture

The HepG2 cell line, a liver hepatocellular carcinoma cell line, was obtained from European Collection of Authenticated Cell Cultures (ECACC) and supplied by Sigma. Cell culture reagents were purchased from Life Technologies (Carlsbad, CA, USA). The cells were grown in complete medium, i.e., Dulbecco's modified Eagle's medium, supplemented with 10% fetal bovine serum (FBS), 2 mmol/L L-glutamine, 100 U/mL penicillin, 100 $\mu\text{g}/\text{mL}$ streptomycin, 250 $\mu\text{g}/\text{mL}$ fungizone and 1 mmol/L sodium pyruvate at 37°C in 5% CO₂ humidified atmosphere. Cells were daily observed under an inverted phase-contrast Eclipse TS100 microscope (Nikon, Tokyo, Japan). For each experiment, cells were allowed to adhere for 24 hr and then medium was replaced with fresh medium containing Cit30 or PEG30 AgNPs. The effects were measured after 24 and 48 hr. Throughout the experiments, cultures were routinely visualized for confluence and cell morphology.

1.4. Exposure and viability assay

Cell viability was determined by the colorimetric 3-(4,5-dimethyl-2-thiazolyl)-2,5-diphenyl tetrazolium bromide (MTT) assay, which measures the formation of purple formazan in viable cells (Twentyman and Luscombe, 1987). Cells were seeded in 96-well plates and after 24 hr, medium was replaced with fresh medium containing coated AgNPs.

Cells were exposed to Cit30 or PEG30 AgNPs at 0, 1, 5, 10, 15, 25 and 50 $\mu\text{g}/\text{mL}$ AgNPs, and to Ag⁺ at 0, 0.5, 0.75, 1, 1.25, 1.5 and 2 $\mu\text{g}/\text{mL}$. Cell viability was measured after 24 hr and 48 hr. Fifty microliters of MTT reagent (1 mg/mL) in phosphate buffered saline (PBS) were added to each well, and incubated for 4 hr at 37°C, 5% CO₂. Medium was then removed, and 150 μL of DMSO were added to each well for crystal solubilization. The optical density of reduced MTT was measured at 570 nm in a microtiter plate reader (Synergy HT Multi-Mode, BioTeK, Winooski, VT), and the cell metabolic activity (MA, a usual marker for cell viability) was calculated as: $MA = ((\text{Sample Abs} - \text{DMSO Abs}) / (\text{Control Abs} - \text{DMSO Abs})) \times 100$. Three independent assays were performed with at least 2 technical replicates each and the results were compared with the control (no exposure). From the MTT results, the IC₅₀ values were similar for Cit30 and for PEG30 around 11 $\mu\text{g}/\text{mL}$ at 24 hr. Therefore, 11 $\mu\text{g}/\text{mL}$ was selected as the higher dose, and a lower dose corresponding to minimal

loss of viability (~IC₁₀, 5 $\mu\text{g}/\text{mL}$) was also selected. The following studies were then performed with cell exposure during 24 hr to 5 $\mu\text{g}/\text{mL}$ and 11 $\mu\text{g}/\text{mL}$ of Cit30 and PEG30 AgNPs.

1.5. Uptake potential by flow cytometry

Uptake potential of Cit30 and PEG30 AgNPs by HepG2 cells was assessed by flow cytometry (FCM), as previously described by Suzuki et al. (2007). Briefly, cells were seeded in 6-well plates and after AgNPs exposure they were trypsinized, collected to FCM tubes and analyzed by FCM. Both parameters, forward scatter (FS), which give information on the particle's size, and side scatter (SS), information on complexity of particles, were measured in a Coulter XL Flow Cytometer (Beckman Coulter, Hialeah, FL, USA) equipped with an argon laser (15 mW, 488 nm). Acquisitions were made using SYSTEM II software v. 3.0 (Beckman Coulter, Hialeah, FL). For each sample, 5000–20,000 cells were analyzed at a flow rate of about 1000 cells/sec.

1.6. Annexin V

Apoptosis and cell viability were measured by FCM in a Coulter XL Flow Cytometer (Beckman Coulter, Hialeah, FL, USA), with the FITC Annexin V Apoptosis Detection Kit (BD Pharmingen, San Diego, CA, USA) according to manufacturer. Briefly, cells were detached and washed with PBS, then cells were resuspended in diluted binding buffer provided with the kit (1:10 in distilled water) at 1×10^6 cells/mL. To stain cell suspension, 5 μL of FITC-Annexin V and 5 μL of propidium iodide. For each sample, 10,000 events were analyzed using the SYSTEM II (v. 2.5) software (Beckman Coulter, Hialeah, FL, USA). The cytogram of FITC fluorescence versus PI fluorescence allows the identification of live intact cells (Annexin V-FITC negative, PI negative), exclusively early apoptotic cells (Annexin V-FITC positive, PI negative), predominantly late apoptotic cells (Annexin V-FITC positive, PI positive), and predominantly necrotic or dead cells (Annexin V-FITC negative, PI positive). FCM data were analyzed by FlowJo software (Tree Star Inc., Ashland, OR).

1.7. Cell cycle and clastogenicity analysis

Cell cycle and putative clastogenic effects were analyzed by flow cytometry according to the method previously described (Oliveira et al., 2014). Briefly, cells were seeded in 6-well plates and after exposure they were washed with PBS, harvested using Trypsin-EDTA and centrifuged twice at 300 $\times g$ for 5 min. Cells were then fixed with 85% cold ethanol and kept at -20°C until analysis. At the time of analysis cells were centrifuged at 300 $\times g$ for 5 min, resuspended in PBS and filtered through a 35- μm nylon mesh to separate aggregates. Then, 50 μL RNase (1 mg/mL) and 50 μL PI (1 mg/mL) were added to each sample which was then incubated for 20 min in darkness at room temperature until analysis. The relative fluorescence intensity of the stained nuclei was measured in a Coulter XL Flow Cytometer (Beckman Coulter, Hialeah, FL, USA) equipped with an argon laser (15 mW, 488 nm). Acquisitions were made using SYSTEM II software v. 3.0 (Beckman Coulter, Hialeah, FL, USA). For each sample, the number of nuclei analyzed was approximately 5000. The percentage of

nuclei in each phase of the cell cycle (G0/G1 — quiescent phase/Gap 1 phase; S — synthesis phase and G2 — Gap 2 phase) was analyzed using the FlowJo software (Tree Star Inc., Ashland, Oregon, USA). In order to assess the putative clastogenic effects of the two coated AgNPs and the silver ion, as described by (Misra and Easton, 1999), the coefficient of variation of the G0/G1 peak was determined.

1.8. Apoptosis and cyclin gene expression

Gene-specific primer pairs (Table 1) were designed using the program Primer3 (Rozen and Skaletsky, 2000) and confirmed for specificity by the UCSC In-Silico PCR Genome Browser (<http://genome.ucsc.edu/cgi-bin/hgPcr>).

Total RNA of control and exposed cells was extracted using the TRIzol method. Organic phase separation was achieved in Phase-Lock Gel Heavy tubes (5 Prime 3 Prime, Inc., Boulder, CO). The aqueous phase was mixed with 70% ethanol and RNA was purified using RNeasy Mini Kit columns (Qiagen, Hilden, Germany). Synthesis of cDNAs was performed by a reverse transcriptase (RT) reaction: 2 µg total RNA were pre-incubated with DNase I (Sigma Aldrich, St. Louis, MO) and reverse-transcribed with 1 µmol/L Oligo dT18, using the Omniscript RT Kit (Qiagen, Hilden, Germany). The cDNA samples were prediluted in ultrapure MilliQ water (1:20). The final individual qPCR reactions contained iQ SYBR Green Supermix (BioRad, Hercules, CA, USA), 0.15 µmol/L each gene-specific primer and 1:4 (V/V) prediluted cDNA (1:20). The qPCR program included 1 min denaturation at 95°C, followed by 40 cycles at 94°C for 5 sec, 58°C for 15 sec, and 72°C for 15 sec. After qPCR, a melting temperature program was performed. At least two technical replicates per sample of qPCR were performed from each of three independent biological replicates. Average PCR and cycle thresholds were determined from the fluorescence data using the algorithm Real-Time PCR Miner (Zhao and Fernald, 2005). Gene expression of BAX (pro-apoptotic gene) and BCL2 (anti-apoptotic gene) and cyclins B1 (CCNB1), and E1 (CCNE1) were normalized with the GAPDH (glyceraldehyde-3-phosphate dehydrogenase gene) reference gene and expressed relative to control cells, calculated from the average efficiencies and cycle thresholds using the Pfaffl method (Pfaffl, 2001).

1.9. Statistical analysis

The results are reported as mean ± standard deviation (SD) of 2 technical replicates in each of the 3 independent experiments.

For MTT assay, the statistical significance between control and exposed cells was performed by one way ANOVA, followed by Dunnett method, a parametric test used when the normality test passed and Dunn's method, a non-parametric test used when the data tested did not pass the normality test. The statistical analysis was performed using Sigma Plot 12.5 software (Systat Software Inc.). For the other assays, the results were compared using two-way ANOVA, followed by Holm-Sidak method as a multiple comparison test, using also Sigma Plot 12.5 software (Systat Software Inc.). The differences were considered statistically significant for $p < 0.05$.

2. Results

2.1. Physicochemical characterization of AgNPs dispersed in water and in cell culture medium

The characteristics of Cit30 and PEG30 AgNPs dispersed in water or in culture medium are summarized in Table 2, including hydrodynamic diameter; polydispersity index (Pdl); zeta potential (ζ); and ionic silver dissolution in ultrapure water and DMEM. The hydrodynamic diameter (Z-average size) in water was above the primary particle size. The values of polydispersity indexes (Pdl) were below 0.3, thus indicating monodisperse distributions. The zeta potential shows that citrate-stabilized NPs carried a strong negative surface charge ($\zeta = 42.7 \pm 2.7$ mV), while the surface of the PEG-stabilized NPs was less negative ($\zeta = 12.1 \pm 0.5$ mV). The release of ionic silver (Ag^+) in DMEM increased to $7.6\% \pm 0.1\%$ at 48 hr of citrate-AgNPs and $7.2\% \pm 0.06\%$ at 48 hr of PEG-AgNPs, which corresponds to an absolute concentration of ≈ 0.836 and ≈ 0.792 µg/mL Ag^+ for the highest concentration used of AgNPs (11 µg/mL).

2.2. Effects on cell growth, morphology and viability

In control conditions, HepG2 cells showed typical morphology (Fig. 1a and d). When they were exposed to Cit30 and PEG30 AgNPs, their confluence decreased, especially for the higher concentration (11 µg/mL) (Fig. 1c and f). No morphological alterations were observed in AgNP-exposed cells, independently of the coating and concentration. The viability of exposed cells was significantly reduced ($p < 0.05$) upon exposure to Cit30 and PEG30 at concentrations higher than 5 µg/mL after 48 hr and 10 µg/mL after 24 hr for Cit30; and

Table 1 – Oligonucleotide primer sequences used for qPCR.

Gene	Forward primer (5'–3')	Reverse primer (5'–3')
BAX ^a	GACGGCCTCCTCTCCTACTT	CAGCCCATCTTCTTCCAGAT
BCL2 ^b	GGAGGATTGTGGCCTTCTTT	GCCGGTTCAGGTAAGTCACTCAGTC
CCNB1 ^c	GCTGAAAATAAGGCCGAAGATCAA	ACCAATGTCCCCAAGAGCTG
CCNE1 ^d	CAGCCTTGGGACAATAATGC	GAGGCTTGCACGTTGAGTTT
GAPDH ^e	ACACCCACTCCTCCACCTT	TACTCCTTGGAGCCATGTG

^a Pro-apoptotic gene.

^b Anti-apoptotic gene.

^c Cyclin B1 gene.

^d Cyclin E1 gene.

^e Glyceraldehyde-3-phosphate dehydrogenase gene.

Table 2 – Physicochemical properties of AgNPs.

	Citrate-AgNPs	PEG-AgNPs
D (nm) ^a	32.7 ± 4.8	31.8 ± 3.2
D (nm) ^b	29.1 ± 3.9	26.8 ± 5.3
D _h (nm) ^c	43.3 ± 0.5	62.1 ± 0.5
PdI ^c	0.25–0.26	0.15–0.16
ζ (mV) ^d	−42.7 ± 2.7	−12.1 ± 0.5
λ _{max} ^e (nm)	408	411
%Ag + in water 0 hr ^f	3.3 ± 0.04	0.63 ± 0.01
%Ag + in DMEM 0 hr ^f	3.8 ± 0.04	3.2 ± 0.03
%Ag + in DMEM 4 hr ^f	5.5 ± 0.07	6.0 ± 0.06
%Ag + in DMEM 24 hr ^f	5.7 ± 0.03	7.0 ± 0.07
%Ag + in DMEM 48 hr ^f	7.6 ± 0.1	7.2 ± 0.06

Standard deviations calculated for D_h, ζ and %Ag + correspond to 3 replicate measurements.

^a Diameter indicated by the manufacturer.

^b Diameter measured by TEM.

^c Hydrodynamic diameter and polydispersity index (PdI) measured by DLS.

^d Zeta potential assessed by electrophoretic mobility (in cell culture medium).

^e Wavelength of maximum absorbance peak in the UV–Vis spectrum.

^f Percentage of ionic silver in the AgNP suspension (10 μg/mL).

concentrations higher than 5 μg/mL after 24 and 48 hr for PEG30 (Fig. 2a–b). Ag⁺ caused a significant decrease in viability at concentrations higher than 0.75 μg/mL and 0.5 μg/mL after 24 and 48 hr, respectively (Fig. 2c).

2.3. Nanoparticle uptake measured by flow cytometry

The uptake of both Cit30 and PEG30 AgNPs by HepG2 cells is shown in Fig. 3. Both concentrations (5 and 11 μg/mL) of both AgNPs induce an increase in side scatter intensity without change of forward scatter intensity of HepG2 cells, which means particles taken up by cells. The uptake potential was significant only for the highest concentration (11 μg/mL) and

no significant difference was observed when comparing cells exposed to Cit30 vs. PEG30 AgNPs.

2.4. Apoptotic markers

The Annexin V assay was performed in order to evaluate the potential of AgNPs to induce apoptosis in HepG2 cells. Although exposure to Cit30 NPs at the IC50 concentration caused a small non-significant increase in the % late apoptotic cells (Fig. 4), there were no statistically significant differences in relation to controls. Both concentration of Cit30 and PEG30 AgNPs decreased the expression levels of selected genes involved in the apoptotic cascade, BCL2 and BAX, after 24 hr (Fig. 5). Cit30 induced a significant decrease of anti-apoptotic BCL2 expression levels for the higher concentration tested and of BAX expression levels for 5 μg/mL. PEG30 induced a significant decrease of BCL2 expression levels for both concentrations used.

2.5. Cell cycle analysis

Fig. 6 shows the effect of Cit30 and PEG30 AgNPs on the cell cycle of HepG2 cells. Cit30 in both doses decreased the percentage of cells in G0/G1 (significant at the higher concentration) and increased the percentage of cells in G2, this effect being visible for both concentrations, but more pronounced for 11 μg/mL ($p < 0.01$) (Fig. 6a). An increase in the percentage of cells in the S phase was also observed for the higher concentration.

PEG30 showed a similar trend, but decreased the percentage of cells at G0/G1 only at the higher concentration (11 μg/mL). The increase of the percentage of cells at G2 and S phases was pronounced at the higher concentration; for the lower concentration, only the populations at G2 increased. The coefficient of variation of the G0/G1 peak did not change significantly with exposure to AgNPs (6 ± 0.3 for 11 μg/mL of citrate-AgNPs and 5 ± 0.54 for 11 μg/mL of PEG-AgNPs), comparatively to their counterparts in the control (5.2 ± 0.98) (Fig. 7). When comparing cell cycle profiles upon exposure to both types of AgNPs, significant

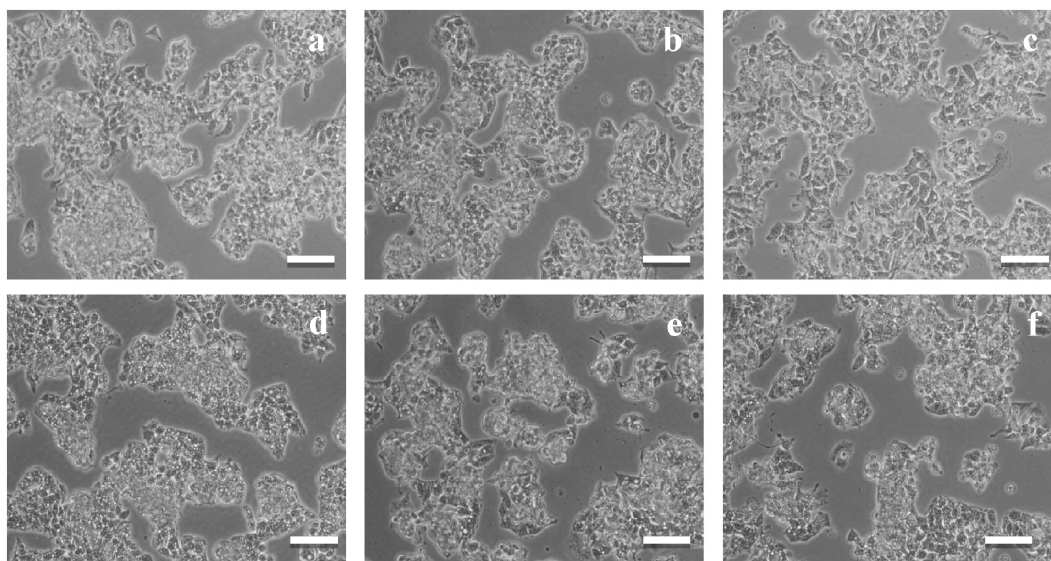


Fig. 1 – Light microscopy images (100X) of HepG2. Cells 24 hr exposed to: (a) 0, (b) 5 μg/mL and (c) 11 μg/mL of citrate-AgNPs; and (d) 0, (e) 5 μg/mL and (f) 11 μg/mL of PEG-AgNPs. Bar corresponds to 100 μm.

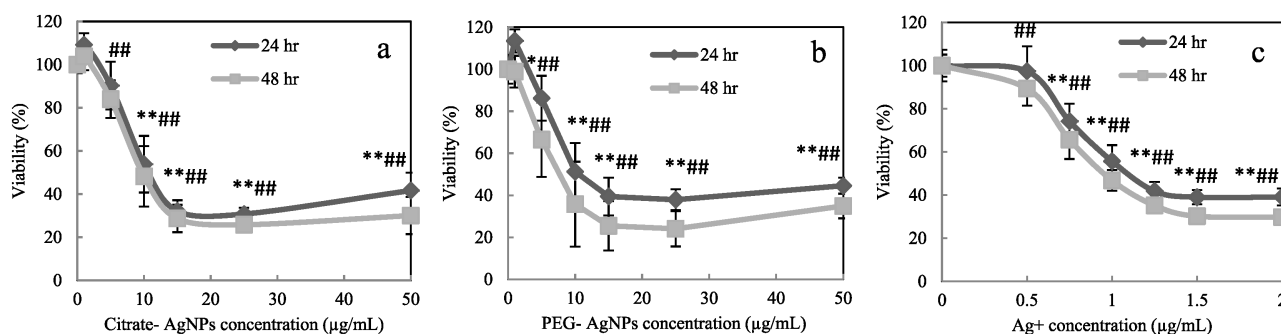


Fig. 2 – Relative cell viability (%) of HepG2. Viability measured by MTT assay, for 24 hr and 48 hr. (a) 30 nm citrate-coated AgNPs; (b) 30 nm PEG coated AgNPs; (c) Ag^+ . Data expressed as mean and standard deviation. * indicate significant differences between control at $p < 0.05$ and ** at $p < 0.01$ for 24 hr; and # indicate significant differences between control at $p < 0.05$ and ## at $p < 0.01$ for 48 hr.

differences were found for the lowest concentration (5 $\mu\text{g/mL}$) at G0/G1 and S phases: the percentage of cells in G0/G1 phase was higher for PEG-AgNPs exposed cells; and the percentage of cells in S phase was higher for the Cit30 AgNPs.

Finally, it should also be stressed that both exposures increased the percentage of subpopulations at channel >600 and channel >800 corresponding to superG2 subpopulations (Fig. 7).

In addition to changing the cell cycle distribution, exposure to AgNPs downregulated the expression of genes involved in G1/S (cyclin E1) and G2/M (cyclin B1) phase transitions (Fig. 8). Both concentrations of Cit30 AgNPs downregulated the expression of cyclin B1 gene (CCNB1), though only significantly for 11 $\mu\text{g/mL}$ ($p < 0.01$). HepG2 cells exposed to PEG30 AgNPs showed a similar profile of CCNB1, where the expression was significantly decreased for 11 $\mu\text{g/mL}$ ($p < 0.01$). In HepG2 exposed to Cit30 the expression of CCNE1 gene was decreased for both concentrations, while cells exposed to PEG30 did not show differences for the higher concentration, showing a significant decrease of CCNE1 expression levels after exposure to 5 $\mu\text{g/mL}$ ($p < 0.05$).

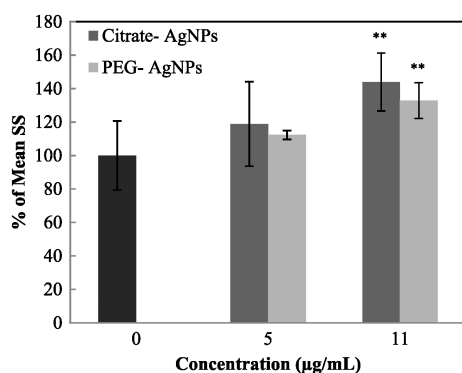


Fig. 3 – Uptake of AgNP by HepG2 cells. The uptake was assessed by the side scattered light through flow cytometry after 24 hr exposure to 5 and 11 $\mu\text{g/mL}$ of citrate-AgNPs and PEG-AgNPs. The results were expressed as the mean \pm SD versus control. ** indicate significant differences between control at $p < 0.01$.

3. Discussion

Citrate-AgNPs are widely used, *e.g.* as antimicrobial agents in industry (Tolaymat et al., 2010), while the use of PEG-coated AgNPs is still emerging, particularly in *e.g.* nanomedical applications (Ginn et al., 2014; Ryan et al., 2008; Thorley and Tetley, 2013). Despite data supporting some cytotoxic effects of AgNPs on different cell lines have been reported, these effects are dependent on multiple aspects such as external factors (*e.g.* storage conditions, dispersion medium) and NP characteristics (*e.g.* size and coating). In particular, research on the coating properties that may confer AgNPs less toxicity is essential, namely the evaluation of cyto- and genotoxic potential.

This study focused on the comparison between citrate- and PEG-coated AgNPs cytotoxicity to human liver cells. As discussed elsewhere (Bastos et al., 2016) coating deeply influences AgNPs physicochemical properties, with citrate coating providing a more negative and, hence, potentially more reactive surface. It has been reported that nanoparticle coating, media composition and ionic strength influences the surface chemistry, shape, aggregation state and dissolution, which can impact toxicological determinations by altering concentration, dissolved ionic silver, aggregation and shape, consequently affecting NP uptake (Tejamaya et al., 2012). The same authors reported that charge-stabilized particles (*e.g.* by citrate) were more unstable and aggregated more than sterically stabilized particles (*e.g.* by PEG); which could induce different levels of cytotoxicity (Wang et al., 2014).

In this study, citrate-coated AgNPs and PEG-coated AgNPs (both 30 nm nanospheres) yielded approximately the same viability profile, up to IC50 concentrations, indicating that particle coating did not greatly influence the AgNPs cytotoxicity potential on HepG2 cell line. We previously evaluated the dissolution rate of Cit30 and PEG30 AgNPs in DMEM medium and found a similar profile of Ag^+ dissolution after 24 and 48 hr (Bastos et al., 2016). Then, we estimated the amount of free Ag^+ dissolved from Cit30 and PEG30 in the culture medium at 10 $\mu\text{g/mL}$ and compared with the toxicity of equivalent Ag^+ from AgNO_3 . For HepG2 the toxicity of Ag^+ from AgNO_3 was lower than the toxicity of AgNPs if we consider only the amount of dissolved Ag^+ . Therefore, we may

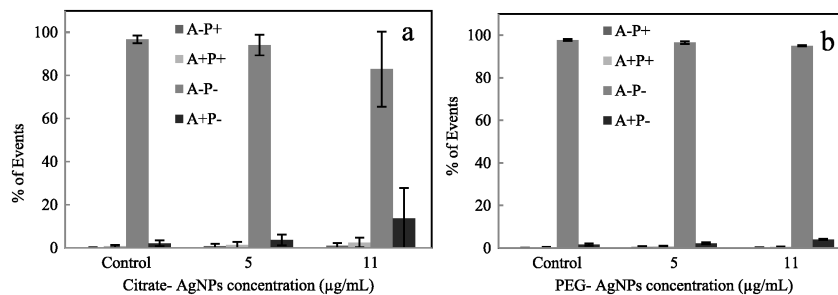


Fig. 4 – Citrate- and PEG-AgNPs apoptotic effects on HepG2. The effects were measured by annexin V assay after 24 hr of exposure to 5 and 11 µg/mL. Intact cells are represented by “A–P–”, dead cells “A–P+”, early apoptotic cells “A+P–” and late apoptotic cells “A+P+”. The results were expressed as the mean ± SD versus control.

postulate that the toxicity of AgNPs is not only due to the dissolved Ag⁺. Accordingly, Gliga et al. (2014) have shown that AgNPs supernatants, containing ionic silver, did not affect cells. Furthermore, the intracellular release of Ag⁺ following cellular uptake, reported as the Trojan horse effect (Hsiao et al., 2015; Park et al., 2010), could be responsible for AgNPs toxicity. Indeed, Cronholm et al. (2013) also suggested that the toxicity mechanisms of silver ion differ from the mechanisms of AgNPs toxicity since this last one is driven by oxidative stress and released silver ions after cellular uptake of the particles.

In our previous study with the keratinocyte cell line HaCaT, Cit30 and PEG30 induced different toxicity profiles, being Cit30 more cytotoxic than PEG30 (Bastos et al., 2016). Also, considering the literature (Caballero-Díaz et al., 2013), it was expected that citrate-AgNPs would induce higher mortality compared to PEG-AgNPs. Lu et al. (2010) found that citrate-coated silver nanopowder was cytotoxic, whereas PVP-coated silver nanoprisms or NPs were not. The authors also highlighted the importance of replacing, in daily life applications, citrate-coating with other biocompatible and

functionalized formulations such as PVP. Pang et al. (2016) demonstrated that the toxicity of AgNPs on murine hepatoma cells (Hepa1c1c7) depended on the surface chemistry of NPs. They suggested that PEG-AgNPs have better biocompatibility, with an optimal biological inertia, and could effectively resist opsonization or non-specific binding to protein in mice. Also, Caballero-Díaz et al. (2013) reported that pegylation of AgNPs reduced cellular uptake and their toxicity to NIH/3T3 (mouse embryonic fibroblasts). Also, when evaluating the uptake rates of gold NPs on human alveolar epithelial cells (A549), Brandenberger et al. (2010) observed that significantly more plain NPs (i.e., stabilized with citrate buffer) could enter the cells than PEG-coated gold NPs. However, from our uptake results there was not a statistical difference between cells exposed to Cit30 AgNPs and cells exposed to PEG30 AgNPs.

We have previously tested these AgNPs in other cell lines and demonstrated that the IC₅₀ for keratinocytes (HaCaT) was 40 µg/mL, above the values herein found for the HepG2 cells. The cytotoxicity of these AgNPs is thus dependent on the cell type, with keratinocytes demonstrating higher tolerance than liver cells. PEG-coated AgNPs induced a similarly decrease on the viability of liver cells (HL-7702) in a dose- and time-dependent manner at doses from 6.25 µg/mL (Song et al., 2012). Faedmaleki et al. (2014) obtained IC₅₀ value of 2.764 µg/mL for HepG2 when exposed to 20–40 nm AgNPs. Similarly, Nowrouzi et al. (2010) obtained IC₅₀ value of 2.75–3 µg/mL for HepG2 after exposure to 5–10 nm AgNPs. However, Xin et al. (2015) observed lower cytotoxicity of 20–50 nm AgNPs to HepG2 cells, where viability decreased with concentrations ranging from 25 to 200 µg/mL. The same authors found a viability decrease of A549 cells after exposure to 20–50 nm AgNPs within concentrations ranging from 12.5 to 200 µg/mL.

Regarding apoptosis, our results did not show significant differences between control and exposed cells after 24 hr. Urbańska et al. (2015) determined the occurrence of apoptosis on glioblastoma multiform (GBM) cells cultured in an *in ovo* model (tumor cell implantation of GBM cells, line U-87, placed on chicken embryo membrane on fertilized chicken eggs in order to study tumors growth rate, angiogenic potential, and metastatic capability) treated with colloidal 70 nm AgNPs (40 µg/mL). Through TUNEL assay, the authors observed no induction of apoptosis as well, despite the increased level of immunohistochemical caspase 3 and 9. The authors suggested that malignant tumor cells, such as GBM, are

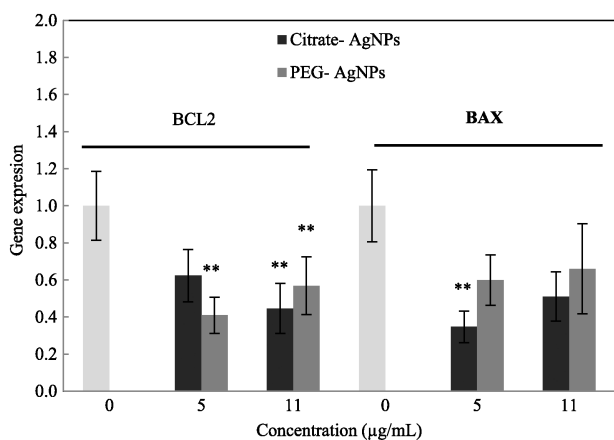


Fig. 5 – HepG2 gene expression of apoptotic genes after 24 hr of AgNPs exposure. (a) Cells exposed to citrate-coated AgNPs; and (b) cells exposed to PEG-coated AgNPs. The results were expressed as mean relative to control cells (normalized with the GAPDH reference gene) and standard deviation. ** indicate significant differences between control at $p < 0.01$.

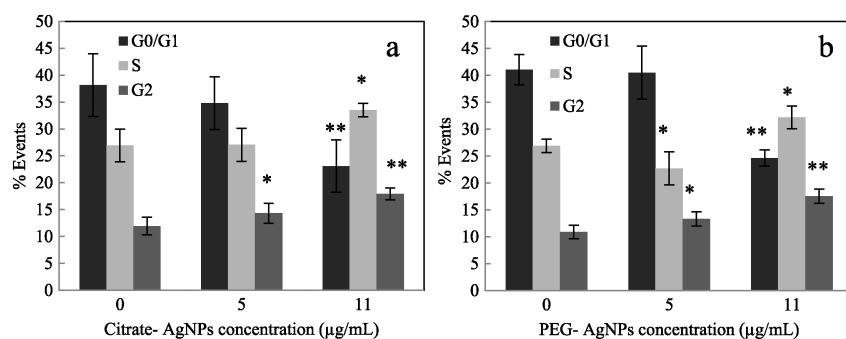


Fig. 6 – Effects of AgNPs on cell cycle dynamics. Cell cycle was analyzed through flow cytometry after exposure to: (a) citrate-coated AgNPs; and (b) PEG-coated AgNPs. The results were expressed as mean and standard deviation. * indicate significant differences between control at $p < 0.05$ and ** at $p < 0.01$.

extremely resistant to apoptosis and particularly resistant to radiation and chemotherapy (Kuriyama et al., 2002). Also, Xue et al. (2016) determined the apoptotic potential of 15 nm AgNPs in HepG2 cells and did not find significant differences between control and 40 µg/mL exposed cells. However, a study using 1 and 50 µmol/L of PVA-AgNPs obtained significant apoptotic effects on HepG2 after 24 hr (Paino and Zucolotto, 2015). In terms of apoptotic gene expression, we have found that both AgNPs downregulated BAX and BCL2 gene expression. Cit30 AgNPs significantly decreased BAX (pro-apoptotic) gene expression for the lowest concentration (5 µg/mL) and BCL2 (anti-apoptotic) gene expression for the higher concentration (11 µg/mL). On the other hand, PEG30 decreased significantly BCL2 gene expression for both concentrations. BCL2 is an anti-apoptotic protein coding gene that prevents the opening of the mitochondrial membrane pore, while BAX — pro-apoptotic coding gene — accelerates it. Mitochondrial membrane pore opening induces the release of cytochrome c from mitochondria. Piao et al. (2011), observed that AgNPs downregulated BCL2 expression and upregulated BAX expression in Human Chang liver cells, resulting in the disruption of mitochondrial membrane potential, followed by cytochrome c release from the mitochondria, resulting in mitochondria-dependent apoptotic pathway. Furthermore, Jeyaraj et al. (2015) found an upregulation of BAX, caspases-6

and -9 and downregulation of BCL-2 on HeLa cells after exposure to AgNPs.

Cell cycle dynamics was evaluated in HepG2 cells exposed to Cit30 and PEG30 AgNPs. For both AgNPs, there were changes on the cell cycle of HepG2 cells. Cit30 and PEG30 induced an increase in the percentage of cells in G2, indicating an arrest at this phase, visible for both concentrations. Also, both AgNPs significantly increased the percentage of cells at S phase for the higher concentration used (11 µg/mL) pointing to an S-phase delay. An S phase delay was also observed by Liu et al. (2010) in HepG2 cells exposed to PVP-coated AgNPs. However, Song et al. (2012) found an increase in the percentage of cells at G2/M phase on HL-7702 cells (human liver cell line) exposed to 100 µg/mL mPEG-SH coated AgNPs after 24 hr. Indeed, cell cycle arrest at G2 was also previously observed as a result of AgNP exposure (AshaRani et al., 2009; Kang et al., 2012; Lee et al., 2011; Wei et al., 2010). Xue et al. (2016) found that no significant changes were observed on HepG2 after exposure to 40 and 80 µg/mL AgNPs for 24 hr. In our study, both exposures promoted the appearance of superG2 subpopulations. This suggests that exposure to AgNPs stimulates the proliferation of the hyperdiploid karyotype subpopulations (ATCC 2015; <http://www.hepg2.com/>) over the typical diploid profile, meaning an increase of the heterogeneity of this culture, and the consequences of this

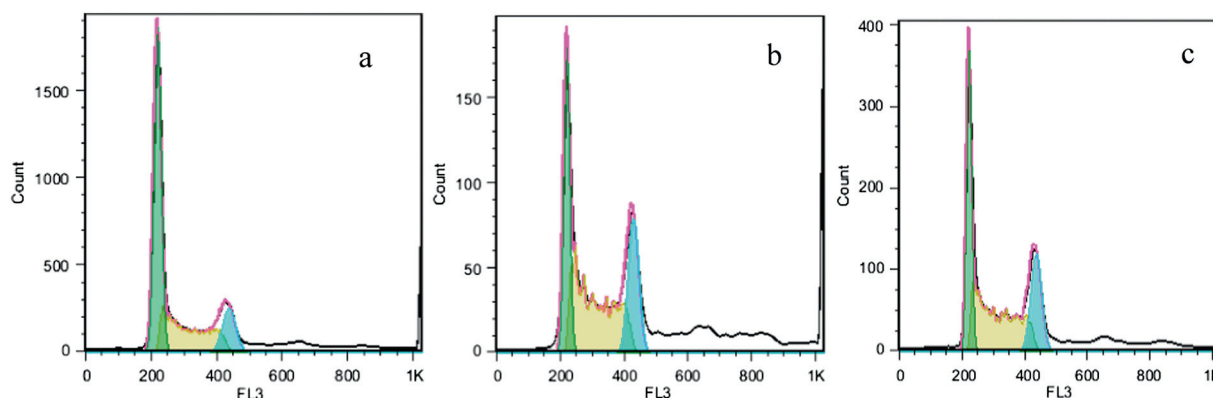


Fig. 7 – Examples of HepG2 cell cycle histograms. The histograms were obtained after 24 hr of AgNPs exposure, measured by flow cytometry. (a) Control; (b) 11 µg/mL of citrate-AgNPs; and (c) 11 µg/mL of PEG-AgNPs.

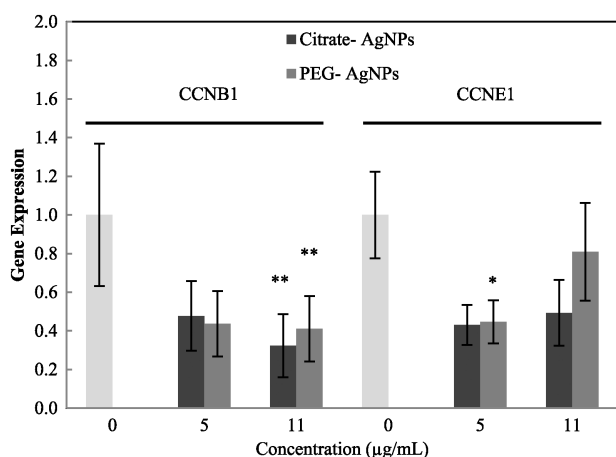


Fig. 8 – HepG2 gene expression of cell cycle genes after 24 hr of AgNPs exposure. (a) Cells exposed to citrate-coated AgNPs; and (b) cells exposed to PEG-coated AgNPs. The results were expressed as mean relative to control cells (normalized with the GAPDH reference gene) and standard deviation. ** indicate significant differences between control at $p < 0.01$ and * $p < 0.05$.

increase remain unknown, as well as the behavior of each subpopulation individually.

Expression of two selected cell cycle regulator genes was also assessed in this study. Cyclin B1, encoded by the *CCNB1* gene, is a regulatory protein which complexes with Cdk1 and both play a determinant role in G2/M phase transition of the cell cycle. Cyclin E1, encoded by the *CCNE1* gene, forms a complex with Cdk2, which accumulates at the G1-S phase and is degraded as cells progress through the S phase. From our results, both AgNPs decreased the *CCNB1* and *CCNE1* gene expression for both concentrations used. *CCNE1* gene expression was decreased after exposure to both AgNPs, especially at the lowest concentration (5 µg/mL), although it was significantly decreased only for PEG-AgNPs. This agrees with the increase in the percentage of cells in S-phase observed for both AgNPs. There are other studies on AgNPs cytotoxicity in agreement with our results: Foldbjerg et al. (2012) found a downregulation of *CCNB1* and *Cdk1* for A549 cell line; and also Asharani et al. (2012) reported a downregulation of *CCNB1* and also of *CCNE1* in normal human lung cells IMR-90 and human brain cancer cells.

4. Conclusions

In sum, our study demonstrates that citrate-coated and PEG-coated AgNPs have similar profiles in decreasing the viability of HepG2 cells. Thus, and contrarily to what we have found in other cell lines such as keratinocytes where citrate coating was generally more toxic, in HepG2 cells the cytotoxicity of AgNPs was independent of the studied coatings. Despite leading to low proliferation, AgNPs did not induced apoptosis for the studied concentrations and the apoptotic related genes *BCL2* and *BAX* were downregulated, supporting that the decrease of proliferation may be due to both cytostatic effects and/or necrotic events.

HepG2 showed the same profile of cell cycle dynamics after exposure to both AgNPs, where, for the higher concentration, there was an increase of the percentage of cells at S and G2 phases. Cyclins gene expressions *CCNB1* and *CCNE1* were also downregulated, which supports cytostatic effects of these coated AgNPs on this cell line. Also, both type of nanoparticles induced higher heterogeneity of the population (increase % of cells at super G2).

This study supports the claim for more thorough studies on different cell lines before a decision can be reached on the toxicity of each type of nanoparticles on humans. For this reason, more research is needed to complement the existing information about the cell lines response to different physicochemical features of AgNPs currently used in industrial, consumer products and nanomedicines.

Acknowledgments

This work was developed in the scope of the projects CICECO-Aveiro Institute of Materials (Ref. FCT UID/CTM/50011/2013) and CESAM (Ref. FCT UID/AMB/50017/2013), financed by national funds through the FCT/MEC and when applicable co-financed by the European Regional Development Fund (FEDER) under the PT2020 Partnership Agreement. Funding to the project FCOMP-01-0124-FEDER-021456 (Ref. FCT PTDC/SAU-TOX/120953/2010) by FEDER through COMPETE and by national funds through FCT, and the FCT-awarded grants (SFRH/BD/81792/2011; SFRH/BPD/111736/2015; SFRH/BPD/74868/2010) are acknowledged. I.F.D and A.L.D.S. acknowledge FCT/MCTES for the research contracts under the Program ‘Investigador FCT’ 2014.

REFERENCES

- Ahlberg, S., Meinke, M.C., Werner, L., Epple, M., Diendorf, J., Blume-Peytavi, U., et al., 2014. Comparison of silver nanoparticles stored under air or argon with respect to the induction of intracellular free radicals and toxic effects toward keratinocytes. *Eur. J. Pharm. Biopharm.* 88 (3), 651–657.
- Asharani, P., Low Kah Mun, G., Hande, M., Valiyaveetil, S., 2009. Cytotoxicity and genotoxicity of silver nanoparticles in human cells. *ACS Nano* 3 (2), 279–290.
- Asharani, P., Sethu, S., Lim, H., Balaji, G., Valiyaveetil, S., Hande, M., 2012. Differential regulation of intracellular factors mediating cell cycle, DNA repair and inflammation following exposure to silver nanoparticles in human cells. *Genome Integr.* 3 (1), 2.
- Bastos, V., de Oliveira, J.F., Brown, D., Johnston, H., Malheiro, E., Daniel-da-Silva, A.L., et al., 2016. The influence of citrate or PEG coating on silver nanoparticle toxicity to a human keratinocyte cell line. *Toxicol. Lett.* 249, 29–41.
- Behra, R., Sigg, L., Clift, M., Herzog, F., Minghetti, M., Johnston, B., et al., 2013. Bioavailability of silver nanoparticles and ions: from a chemical and biochemical perspective. *J. R. Soc. Interface* 10 (87), 20130396.
- Boonkaew, B., Kempf, M., Kimble, R., Cuttle, L., 2014. Cytotoxicity testing of silver-containing burn treatments using primary and immortal skin cells. *Burns* 40 (8), 1562–1569.
- Brandenberger, C., Mühlfeld, C., Ali, Z., Lenz, A.G.G., Schmid, O., Parak, W.J., et al., 2010. Quantitative evaluation of cellular uptake and trafficking of plain and polyethylene glycol-coated gold nanoparticles. *Small* 6 (15), 1669–1678.

- Caballero-Díaz, E., Pfeiffer, C., Kastl, L., Gil, P., Simonet, B., Valcárcel, M., et al., 2013. The toxicity of silver nanoparticles depends on their uptake by cells and thus on their surface chemistry. *Part. Syst. Charact.* 30 (12), 1079–1085.
- Chen, L.Q., Fang, L., Ling, J., Ding, C.Z., Kang, B., Huang, C.Z., 2015. Nanotoxicity of silver nanoparticles to red blood cells: size dependent adsorption, uptake, and hemolytic activity. *Chem. Res. Toxicol.* 28 (3), 501–509.
- Comfort, K.K., Maurer, E.I., Hussain, S.M., 2014. Slow release of ions from internalized silver nanoparticles modifies the epidermal growth factor signaling response. *Colloids Surf. B: Biointerfaces* 123, 136–142.
- Cronholm, P., Karlsson, H.L., Hedberg, J., Lowe, T.A., Winnberg, L., Elihn, K., et al., 2013. Intracellular uptake and toxicity of Ag and CuO nanoparticles: a comparison between nanoparticles and their corresponding metal ions. *Small* 9 (7), 970–982.
- Dusinska, M., Magdolenova, Z., Fjellsbø, L.M., 2013. Toxicological aspects for nanomaterial in humans. *Methods Mol. Biol.* 1–12.
- Eckhardt, S., Brunetto, P., Gagnon, J., Priebe, M., Giese, B., Fromm, K., 2013. Nanobio silver: its interactions with peptides and bacteria, and its uses in medicine. *Chem. Rev.* 113 (7), 4708–4754.
- Faedmaleki, F., H Shirazi, F., Salarian, A.A., Ahmadi Ashtiani, H., Rastegar, H., 2014. Toxicity effect of silver nanoparticles on mice liver primary cell culture and HepG2 cell line. *Iran. J. Pharm. Res.* 13 (1), 235–242.
- Fernández-López, C., Mateo-Mateo, C., Alvarez-Puebla, R., Pérez-Juste, J., Pastoriza-Santos, I., Liz-Marzán, L., 2009. Highly controlled silica coating of PEG-capped metal nanoparticles and preparation of SERS-encoded particles. *Langmuir* 25 (24), 13894–13899.
- Franci, G., Falanga, A., Galdiero, S., Palomba, L., Rai, M., Morelli, G., et al., 2015. Silver nanoparticles as potential antibacterial agents. *Molecules* 20 (5), 8856–8874.
- Foldbjerg, R., Irving, E., Hayashi, Y., Sutherland, D., Thorsen, K., Autrup, H., Beer, C., 2012. Global gene expression profiling of human lung epithelial cells after exposure to nanosilver. *Toxicol. Sci.* 130, 145–157.
- Ginn, C., Khalili, H., Lever, R., Brocchini, S., 2014. PEGylation and its impact on the design of new protein-based medicines. *Future Med. Chem.* 6 (16), 1829–1846.
- Gluga, A., Skoglund, S., Odnevall Wallinder, I., Fadeel, B., Karlsson, H., 2014. Size-dependent cytotoxicity of silver nanoparticles in human lung cells: the role of cellular uptake, agglomeration and Ag release. *Part. Fibre Toxicol.* 11 (1), 1.
- Gutierrez, L., Aubry, C., Cornejo, M., Croue, J.P., 2015. Citrate-coated silver nanoparticles interactions with effluent organic matter: influence of capping agent and solution conditions. *Langmuir* 31 (32), 8865–8872.
- Hsiao, I.L.L., Hsieh, Y.K.K., Wang, C.F.F., Chen, I.C.C., Huang, Y.J.J., 2015. Trojan-horse mechanism in the cellular uptake of silver nanoparticles verified by direct intra- and extracellular silver speciation analysis. *Environ. Sci. Technol.* 49, 3813–3821.
- Jain, A., Jain, S.K., 2008. PEGylation: an approach for drug delivery. A review. *Crit. Rev. Ther. Drug Carrier Syst.* 25 (5), 403–447.
- Jeyaraj, M., Renganathan, A., Sathishkumar, G., 2015. Biogenic metal nanoformulations induce Bax/Bcl2 and caspase mediated mitochondrial dysfunction in human breast cancer cells (MCF 7). *RSC Adv.* 5 (3), 2159–2166.
- Kang, S., Lee, Y., Lee, E.-K., Kwak, M.-K., 2012. Silver nanoparticles-mediated G2/M cycle arrest of renal epithelial cells is associated with NRF2-GSH signaling. *Toxicol. Lett.* 211 (3), 334–341.
- Kennedy, D.C., Orts-Gil, G., Lai, C.H., Müller, L., Haase, A., Luch, A., et al., 2014. Carbohydrate functionalization of silver nanoparticles modulates cytotoxicity and cellular uptake. *J. Nanobiotechnol.* 12 (1), 59.
- Kim, T.H., Kim, M., Park, H.S., Shin, U.S., Gong, M.S., Kim, H.W., 2012. Size-dependent cellular toxicity of silver nanoparticles. *J. Biomed. Mater. Res. A* 100 (4), 1033–1043.
- Kuriyama, H., Lamborn, K.R., O'Fallon, J.R., Iturria, N., Sebo, T., Schaefer, P.L., et al., 2002. Prognostic significance of an apoptotic index and apoptosis/proliferation ratio for patients with high-grade astrocytomas. *Neuro-Oncology* 4 (3), 179–186.
- Lee, Y., Kim, D., Oh, J., Yoon, S., Choi, M., Lee, S., et al., 2011. Silver nanoparticles induce apoptosis and G2/M arrest via PKC ζ -dependent signaling in A549 lung cells. *Arch. Toxicol.* 85 (12), 1529–1540.
- Liu, W., Wu, Y., Wang, C., Li, H., Wang, T., Liao, C., et al., 2010. Impact of silver nanoparticles on human cells: effect of particle size. *Nanotoxicology* 4 (3), 319–330.
- Lu, W., Senapati, D., Wang, S., Tovmachenko, O., Singh, A.K., Yu, H., et al., 2010. Effect of surface coating on the toxicity of silver nanomaterials on human skin keratinocytes. *Chem. Phys. Lett.* 487 (1), 92–96.
- McShan, D., Ray, P.C., Yu, H., 2014. Molecular toxicity mechanism of nanosilver. *J. Food Drug Anal.* 22 (1), 116–127.
- Misra, R., Easton, M., 1999. Comment on analyzing flow cytometric data for comparison of mean values of the coefficient of variation of the G1 peak. *Cytometry* 36 (2), 112–116.
- Nowack, B., Bucheli, T., 2007. Occurrence, behavior and effects of nanoparticles in the environment. *Environ. Pollut.* 150 (1), 5–22.
- Nowrouzi, A., Meghraz, K., Golmohammadi, T., Golestani, A., Ahmadian, S., Shafieezadeh, M., et al., 2010. Cytotoxicity of subtoxic AgNP in human hepatoma cell line (HepG2) after long-term exposure. *Iran. Biomed. J.* 14 (1/2), 23–32.
- Oliveira, H., Monteiro, C., Pinho, F., Pinho, S., Ferreira de Oliveira, J.M., Santos, C., 2014. Cadmium-induced genotoxicity in human osteoblast-like cells. *Mutat. Res. Genet. Toxicol. Environ. Mutagen.* 775–776, 38–47.
- Paino, I.M.M.M., Zucolotto, V., 2015. Poly(vinyl alcohol)-coated silver nanoparticles: activation of neutrophils and nanotoxicology effects in human hepatocarcinoma and mononuclear cells. *Environ. Toxicol. Pharmacol.* 39 (2), 614–621.
- Pang, C., Brunelli, A., Zhu, C., Hristozov, D., Liu, Y., Semenzin, E., et al., 2016. Demonstrating approaches to chemically modify the surface of Ag nanoparticles in order to influence their cytotoxicity and biodistribution after single dose acute intravenous administration. *Nanotoxicology* 10 (2), 129–139.
- Park, E.J.J., Yi, J., Kim, Y., Choi, K., Park, K., 2010. Silver nanoparticles induce cytotoxicity by a Trojan-horse type mechanism. *Toxicol. in Vitro* 24, 872–878.
- Park, J., Lim, D.-H.H., Lim, H.-J.J., Kwon, T., Choi, J.-s.S., Jeong, S., et al., 2011. Size dependent macrophage responses and toxicological effects of Ag nanoparticles. *Chem. Commun. (Camb.)* 47 (15), 4382–4384.
- Pfaffl, M., 2001. A new mathematical model for relative quantification in real-time RT-PCR. *Nucleic Acids Res.* 29 (9), e45–e45.
- Piao, M.J., Kang, K.A., Lee, I.K., Kim, H.S., Kim, S., Choi, J.Y., et al., 2011. Silver nanoparticles induce oxidative cell damage in human liver cells through inhibition of reduced glutathione and induction of mitochondria-involved apoptosis. *Toxicol. Lett.* 201 (1), 92–100.
- Pillai, Z.S., Kamat, P.V., 2004. What factors control the size and shape of silver nanoparticles in the citrate ion reduction method? *J. Phys. Chem. B* 108 (3), 945–951.
- Rai, M., Ingle, A.P., Birla, S., Yadav, A., Santos, C.A., 2015. Strategic role of selected noble metal nanoparticles in medicine. *Crit. Rev. Microbiol.* 1–24.
- Roberts, S.M., James, R.C., Williams, P.L., 2014. Principles of Toxicology: Environmental and Industrial Applications. John Wiley & Sons.
- Rozen, S., Skaletsky, H., 2000. Primer3 on the WWW for general users and for biologist programmers. *Methods Mol. Biol.* 132, 365–386.
- Ryan, S.M.M., Mantovani, G., Wang, X., Haddleton, D.M., Brayden, D.J., 2008. Advances in PEGylation of important biotech molecules: delivery aspects. *Expert Opin. Drug Deliv.* 5 (4), 371–383.

- Sharma, V., Yngard, R., Lin, Y., 2009. Silver nanoparticles: green synthesis and their antimicrobial activities. *Adv. Colloid Interf. Sci.* 145 (1), 83–96.
- Song, X.-l., Li, B., Xu, K., Liu, J., Ju, W., Wang, J., et al., 2012. Cytotoxicity of water-soluble mPEG-SH-coated silver nanoparticles in HL-7702 cells. *Cell Biol. Toxicol.* 28 (4), 225–237.
- Suzuki, H., Toyooka, T., Ibuki, Y., 2007. Simple and easy method to evaluate uptake potential of nanoparticles in mammalian cells using a flow cytometric light scatter analysis. *Environ. Sci. Technol.* 41 (8), 3018–3024.
- Tejamaya, M., Römer, I., Merrifield, R., Lead, J., 2012. Stability of citrate, PVP, and PEG coated silver nanoparticles in ecotoxicology media. *Environ. Sci. Technol.* 46 (3), 7011–7017.
- Thorley, A.J., Tetley, T.D., 2013. New perspectives in nanomedicine. *Pharmacol. Ther.* 140 (2), 176–185.
- Tolaymat, T.M., El Badawy, A.M., Genaidy, A., Scheckel, K.G., Luxton, T.P., Suidan, M., 2010. An evidence-based environmental perspective of manufactured silver nanoparticle in syntheses and applications: a systematic review and critical appraisal of peer-reviewed scientific papers. *Sci. Total Environ.* 408 (5), 999–1006.
- Twentyman, P., Luscombe, M., 1987. A study of some variables in a tetrazolium dye (MTT) based assay for cell growth and chemosensitivity. *Br. J. Cancer* 56 (3), 279–285.
- Urbańska, K., Pająk, B., Orzechowski, A., 2015. The effect of silver nanoparticles (AgNPs) on proliferation and apoptosis of in ovo cultured glioblastoma multiforme (GBM) cells. *Nanoscale Res. Lett.* 10 (1), 1–11.
- Wang, X., Ji, Z., Chang, C., Zhang, H., Wang, M., Liao, Y.-P., et al., 2014. Use of coated silver nanoparticles to understand the relationship of particle dissolution and bioavailability to cell and lung toxicological potential. *Small* 10 (2), 385–398.
- Wei, L., Tang, J., Zhang, Z., Chen, Y., Zhou, G., Xi, T., 2010. Investigation of the cytotoxicity mechanism of silver nanoparticles in vitro. *Biomed. Mater.* 5 (4), 44103.
- Xin, L., Wang, J., Fan, G., Che, B., Wu, Y., Guo, S., et al., 2015. Oxidative stress and mitochondrial injury-mediated cytotoxicity induced by silver nanoparticles in human A549 and HepG2 cells. *Environ. Toxicol.*
- Xue, Y., Zhang, T., Zhang, B., Gong, F., Huang, Y., Tang, M., 2016. Cytotoxicity and apoptosis induced by silver nanoparticles in human liver HepG2 cells in different dispersion media. *J. Appl. Toxicol.* 36 (3), 352–360.
- Zhang, F., Durham, P., Sayes, C.M., Lau, B.L., Bruce, E.D., 2015. Particle uptake efficiency is significantly affected by type of capping agent and cell line. *J. Appl. Toxicol.* 35 (10), 1114–1121.
- Zhang, T., Wang, L., Chen, Q., Chen, C., 2014. Cytotoxic potential of silver nanoparticles. *Yonsei Med. J.* 55 (2), 283–291.
- Zhao, S., Fernald, R.D., 2005. Comprehensive algorithm for quantitative real-time polymerase chain reaction. *J. Comput. Biol.* 12 (8), 1047–1064.